R E P O R T S

meridional transects for PCO$_2$ measurements made during each event are also indicated. June 1982 to June 1983 (intense event, 1 transect); August 1986 to July 1987 (medium, 7 transects); October 1991 to May 1992 (marginal intensity, 2 transects); October 1992 to October 1993 (marginal, 3 transects); April 1994 to June 1995 (marginal, 8 transects); and April 1997 to April 1998 (intense, 15 transects).

12. To test biases caused by undersampling, we computed time trends of SST using the regularly spaced monthly mean values extracted from the compilation of Reynolds *et al.* (*13*) for the non–El Niño periods (*11*) in the Niño 3.4 area. The SST trends thus computed are compared with those computed using our limited SST values measured concurrently with PCO$_2$. They are found to be in agreement within 1 SD, indicating that the time trends computed with our limited number and irregular spacing of measurements are consistent with those obtained with the full set of the SST data. For example, for the post-1990 trend, the full data yield $-0.14° \pm 0.02°$C year^{-1} ($n = 87$), which compares with $-0.12° \pm 0.06°$C year^{-1} ($n = 32$) for the most consistent case; and for the post-1992 trend, the full data yield $-0.11° \pm 0.11°$C year^{-1} ($n = 66$), which compares with $+0.01° \pm 0.09°$C year^{-1} ($n = 26$) for one of the least consistent cases.

13. R. W. Reynolds, N. A. Rayner, T. M. Smith, D. C. Stokes, W. Wang, "NOAA optimum interpolation (OI) sea surface temperature (SST) V2" (2003) (available at ftp://ftpprd.ncep.noaa.gov/pub/cmd/sst/papers/oiv2pap/).

14. C. Marzban, J. T. Schaefer, *Mon. Weather Rev.* **129**, 884 (2001).

15. W. H. Press, B. P. Flannery, S. A. Teukolsky, W. T. Vetterling, *Numerical Recipes* (Cambridge Univ. Press, Cambridge, 1986), pp. 491–494.

16. |Z| values greater than 2.575 indicate sufficient evidence for claiming that the test is valid with a greater than 99% probability.

17. T. Takahashi, J. Olafsson, J. Goddard, D. W. Chipman, S. C. Sutherland, *Global Biogeochem. Cycles* **7**, 843 (1993).

18. *GLOBALVIEW-CO2: Cooperative Atmospheric Data Integration Project—Carbon Dioxide*. (CD-ROM, NOAA Climate Monitoring and Diagnostics Laboratory, Boulder, Colorado, 2001) (also available on Internet via anonymous FTP to ftp.cmdl.noaa.gov. Path: ccg/co2/GLOBALVIEW).

19. R. L. Borgne, R. A. Feely, D. J. Mackey, *Deep-Sea Res. II* **49**, 2425 (2002).

20. T. P. Guilderson, D. P. Schrag, *Science* **281**, 240 (1998).

21. D. Gu, S. G. H. Philander, *Science* **275**, 805 (1997).

22. M. J. McPhaden, D.-X. Zhang, *Nature* **415**, 603 (2002).

23. N. Schneider, A. J. Miller, M. A. Alexander, C. Deser, *J. Phys. Oceanogr.* **29**, 1056 (1999).

24. J. E. Dore, R. Lukas, D. W. Sadler, D. M. Karl, *Nature* **424**, 764 (2003).

25. D. E. Archer *et al.*, *Deep-Sea Res. II* **43**, 779 (1996).

26. R. Wanninkhof, K. Thoning, *Mar. Chem.* **44**, 189 (1993).

27. N. R. Bates, T. Takahashi, D. W. Chipman, A. H. Knapp, *J. Geophys. Res.* **103**, 15567 (1998).

28. D. W. Chipman, J. Marra, T. Takahashi, *Deep-Sea Res.* **40**, 151 (1993).

29. Supported by grants from NOAA, NASA, and Ford Motor Company (T.T.), and from NOAA (R.A.F.) for field operations. We thank R. Wanninkhof of NOAA and H. Y. Inoue of the Japan Meteorological Research Institute for providing data; D. Martinson of LDEO and C. Marzban of the Department of Statistics, University of Washington, Seattle, for advice on statistics; and B. Linsley of the State University of New York at Albany for critical reading of the manuscript. This is LDEO contribution no. 6500, PMEL contribution no. 2579, and University of Washington and Joint Institute for the Study of the Atmosphere and Ocean contribution no. 1021.

30 June 2003; accepted 23 September 2003

Larsen Ice Shelf Has Progressively Thinned

Andrew Shepherd,[1]* Duncan Wingham,[2] Tony Payne,[3] Pedro Skvarca[4]

The retreat and collapse of Antarctic Peninsula ice shelves in tandem with a regional atmospheric warming has fueled speculation as to how these events may be related. Satellite radar altimeter measurements show that between 1992 and 2001 the Larsen Ice Shelf lowered by up to 0.27 ± 0.11 meters per year. The lowering is explained by increased summer melt-water and the loss of basal ice through melting. Enhanced ocean-driven melting may provide a simple link between regional climate warming and the successive disintegration of sections of the Larsen Ice Shelf.

On average, Antarctic Peninsula (AP) ice shelves have retreated by ~300 km^2 each year since 1980 (*1*). This gradual retreat has been punctuated by two catastrophic collapses, in January 1995 (*2*) and February 2002, when the remaining northern sections of the Larsen Ice Shelf (LIS) (Fig. 1) fragmented into icebergs. In contrast to the prolonged retreats, these 2000- and 3250-km^2 ice-shelf sections—Larsen-A and Larsen-B—disintegrated over days or weeks. Although the initial retreats of their ice fronts may have resulted from iceberg calving beyond stable geometrical posi-

tions (*3*), it is not clear that this explains the wholesale disintegration of large ice-shelf sections. Speculation as to the mechanism that caused the final collapses has concentrated on the destabilizing effects of increased surface melt-water (*4–6*), which may have enhanced the process of crevasse fracture (*7*). Although that mechanism provides a link between the regional climate warming and the breakup of ice shelves at the AP, direct observations are insufficient to determine the importance of ice-shelf stability criteria or the impact of increased surface melt. Here, we show that the LIS may have become susceptible to crevasse fracture through a sustained ice thinning.

We used 9 years of European Remote Sensing (ERS-1 and ERS-2) satellite radar altimeter measurements to determine the surface elevation change of the LIS since 1992. Ice-shelf surface elevation was calculated relative to the WGS 84 Earth ellipsoid at each individual crossing point of the satellite ground track during 35-day orbit repeat cycles (*8*). From these data, we

formed 45 time series of elevation change (e.g., Fig. 2) across the LIS at the finest resolution afforded by the ERS altimeters (*9*). The ERS ground tracks provided a mean crossing point separation of 14 km, and the precise location of the ~10-km altimeter footprint drifted by less than 1.2 km through time as a result of orbit maneuvers. We detected no radar penetration of the LIS surface at any time (*10*), and we removed the ocean tide from each elevation time series using predictions of ice-shelf tidal displacement (*11*). We calculated the trend of elevation change at each crossing point from the tide-adjusted time series and interpolated these data using a quintic triangulation scheme (Fig. 1).

Between 1992 and 2001 the mean rates of elevation change of the Larsen-B and -C ice shelves were -0.17 ± 0.11 and -0.08 ± 0.04 m yr^{-1}, respectively. In general, the northernmost sections of the Larsen-C experienced the greatest decrease in surface elevation, with a peak rate of lowering of 0.27 ± 0.11 m yr^{-1} some 80 km west of the Larsen meteorological station (Fig. 1). Toward the southern tip of Larsen-C, one time series showed that the ice shelf thickened at the terminus of the Lurabee Glacier (69.25°S, 63.62°W), where ice is discharged from Palmer Land. Recent radar, seismic, and Global Positioning System elevation surveys (*12*) show that sections of the Larsen-B lowered relative to the geoid by 0.18 m yr^{-1} between 1991 and 1999, in agreement with our satellite-derived rate.

The rate of elevation change of a floating ice-shelf surface relative to the ellipsoid ($\partial h/\partial t$) is due to fluctuations in sea-level height (Δ_s), ocean (ρ_w) and ice-shelf (ρ_f) densities, net surface ($\dot{M}_s$) and basal ($\dot{M}_b$) mass accumulation, and ice-flux di-

[1]Centre for Polar Observation and Modelling, Scott Polar Research Institute, University of Cambridge, Cambridge CB2 1ER, UK. [2]Centre for Polar Observation and Modelling, University College London, Gower Street, London WC1E 6BT, UK. [3]Centre for Polar Observation and Modelling, University of Bristol, University Road, Bristol BS8 1SS, UK. [4]Instituto Antártico Argentino, Cerrito 1248, 1010 Buenos Aires, Argentina.

*To whom correspondence should be addressed. E-mail: aps46@cam.ac.uk

vergence ($M\nabla.v$). For an ice column in hydrostatic equilibrium with no vertical ice shear, $\partial h/\partial t$ can be written as

$$\frac{\partial h}{\partial t} = \frac{\partial \Delta_s}{\partial t} - M\frac{\partial}{\partial t}\left(\frac{1}{\rho_w}\right) + \int_0^M dm\frac{\partial}{\partial t}\left(\frac{1}{\rho_f(m)}\right) +$$

$$\left(\frac{1}{\rho_{ice} - \rho_w}\right)(\dot{M}_s + \dot{M}_b + M\nabla.v) \qquad (1)$$

where ρ_{ice} is the density of ice (917 kg m^{-3}) and M is the ice-shelf mass per unit area. We investigated trends and variability in each component of Eq. 1 to determine the origin of the LIS surface lowering.

External contributions to $\partial h/\partial t$ include sea level and density. Although eustatic sea level has risen by only 2 mm yr^{-1} in the 20th century (13), atmospheric pressure fluctuations occur (14) that could lead to a 9-year uncertainty in Δ_s of up to 11 mm yr^{-1}. Tide model inaccuracies introduce a further 26 mm yr^{-1} uncertainty. Oceanographic records show that seasonal and interannual variations in salinity (15) modify ρ_w, resulting in up to 10 mm yr^{-1} uncertainty in elevation change. In addition, nearby deep and surface layers of the Weddell Sea have warmed by 0.01°C yr^{-1} for several decades (16, 17), and a similar warming (or cooling) of the water beneath the LIS could raise (or lower) the ice shelf at a rate of 15 mm yr^{-1}. We estimate the combined uncertainty resulting from these contributions to be 34 mm yr^{-1}, a value that is small when compared with the observed trend. The LIS lowering must reflect a change in the ice shelf itself.

We investigated the possibility that the LIS $\partial h/\partial t$ may have resulted from a mass-conservative densification of the ice shelf (the third term in Eq. 1). The gradually warming (18) and lengthening (19) summer climate may have accelerated firn densification during the interval of the measurement. To bound this acceleration, we estimated an initial LIS firn density (20) and supposed that the entire upper 8 m of firn layer (beneath which interannual temperature changes do not penetrate) (12) were densified to ice. This calculation leads to rates of elevation change of −0.12 and −0.28 m yr^{-1} at the Larsen-B and -C, respectively, the difference reflecting the lower initial density of the colder Larsen-C. These changes are comparable to the observed lowering (Fig. 1), and densification cannot be excluded as the sole explanation of the lowering. However, the energy available for thermally driven firn densification is limited by air temperature (1) and melt-season duration (19), which decrease southward. We used observed ablation measurements and a positive degree-day model (21) to estimate the change in summer melt-water production

(22). Assuming the increased melt-water is entirely retained at the density of ice, the estimated contribution to $\partial h/\partial t$ was −0.07 and −0.05 m yr^{-1} at the Larsen-B and -C, respectively. To assign all of the observed lowering of the Larsen-C to densification makes a heavy demand on melt-water production (Fig. 3) at the northern Larsen-C.

To investigate further, we examined in detail airborne measurements of Larsen-C ice thickness that have been ongoing for several decades (23). These data show that the Larsen-C has thinned at an average rate of 0.29 ± 0.68 m yr^{-1} since 1966 (24). Although the aircraft data are sparse and uncertain, this rate shows that the thinning predates

for several decades that observed more precisely by the satellite. Allocating this rate to densification, for which the thinning rate equals the elevation rate relative to sea level, appears incompatible with the trend in melt-water production (22). Our conclusion is that, for Larsen-C at least, some other cause of thinning is present as well.

The remaining terms in Eq. 1 are mass losses. A 10% century^{-1} increase in snow accumulation ($\dot{M}_s$) similar to that recorded nearby at the ~2000-m altitude Dyer Plateau (25) would increase surface elevation by some 2 mm yr^{-1}. Fluctuations occur at shorter time scales (8), but snow-pit measurements at Larsen-B show that accumulation has remained close to
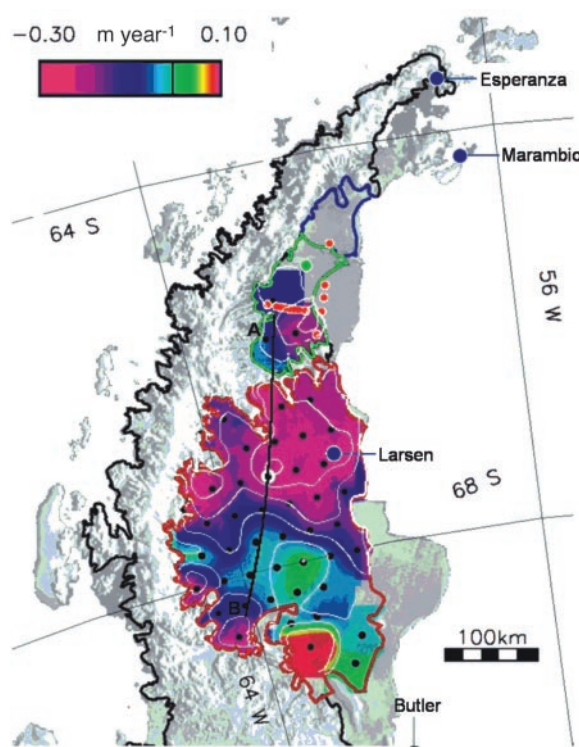

Fig. 1. Rate of surface elevation change of the Larsen Ice Shelf determined from ERS radar altimeter measurements recorded between 1992 and 2001 (color scale and 0.1 m yr^{-1} white contours). The elevation data are superimposed on a mosaic of Advanced Very-High-Resolution radiometer (AVHRR) satellite imagery (gray scale) (38), and data points used in the interpolation are shown as black dots. Also shown are the locations of meterological stations (blue dots) and stakes used to measure changes in snow height (red dots) and surface mass balance (5-km grid, centered at green dot). The 1990 boundaries of the Larsen-A, -B, and -C ice-shelf sections are highlighted with blue, green, and red borders, respectively. Larsen-A collapsed before the ERS measurements; Larsen-B has since disintegrated; Larsen-C remains intact.
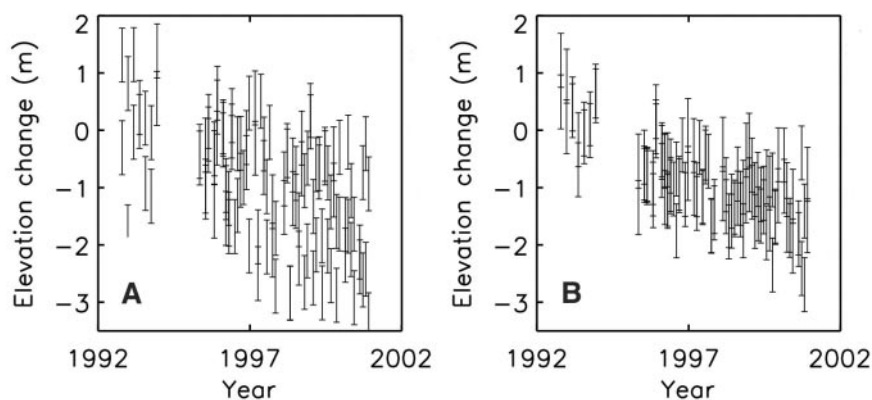

Fig. 2. Change in surface elevation between 1992 and 2001 recorded by the ERS radar altimeters ~80 km west of the Larsen meteorological station (see Fig. 1) at the Larsen-C ice shelf before (**A**) and after (**B**) removal of the periodic signal of ocean tide (11). On average, the tide correction reduced the variability in the trends from 0.4 to 0.2 m yr^{-1}. The location of this time series is highlighted with a white border in Fig. 1.

the long-term average (26), with a 9-year variability of 31 mm yr^{-1}. Turning to the mass supply (M), reduced glacier influx must have occurred for the advection time scale of 10^2 to 10^3 years to affect the entire LIS. However, ice-core records show no accumulation deficit within the catchment basins of tributary glaciers (25), and there is no reason to suppose that these glaciers have thinned. It is possible that a warming of the shelf interior, or a reduction in stress at pinning points, may have disturbed the LIS force balance (3) and thus $\nabla.v$. We constructed a two-dimensional model of the LIS based on the standard rheology equations and momentum and mass-continuity equations (27, 28), to determine, as an example, the effect of a decrease in ice-shelf viscosity. We determined the thinning associated with a 2°C warming penetrating to different depths, and the maximum lowering rate that could be attained was 8 mm yr^{-1}, because of the slow response to changes in the force balance. The combined uncertainty of all of these estimates is 32 mm yr^{-1}. Any LIS mass imbalance must have arisen through basal melting ($\dot{M}_b$).
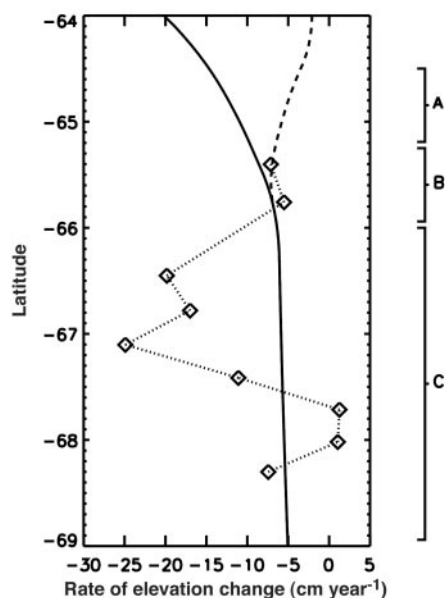

Fig. 3. Larsen Ice Shelf (LIS) surface elevation change (diamonds) along transect A-B (Fig. 1), compared with the estimated change due to increased melt-water production (22). The model assumes that melt-water mass is conserved by the shelf (solid line) until an initial 8-m layer densifies to ice, in which case the excess is supposed to run off (dashed line). No runoff occurs from the LIS section included in our satellite data set. Although stake measurements at Larsen-B (see Fig. 1) show large increases in surface melting—in line with the model prediction—they say nothing about conditions farther south. Our data show that a 31,000-km^2 region of the LIS between 65.5°S and 67.5°S lowered by 0.08 ± 0.03 m yr^{-1} more than the rate expected from densification, equivalent to the freeboard expression of a 21 ± 8 gigaton yr^{-1} loss of ice mass.

Although basal melting rates under the LIS are uncertain and their fluctuation even more so, the conclusion that basal melting has been and is thinning the LIS, at an average rate our measurement and estimate of the effect of densification (Fig. 3) put at 0.78 m yr^{-1}, is not unreasonable given the oceanographic data. Beneath the nearby Filchner-Ronne Ice Shelf (FRIS), melt rates are typically 0.19 m yr^{-1} (29), but substantially greater melt occurs in regions where warm waters are transported beneath floating ice (30). Basal melt rates of 2 to 3 m yr^{-1} are observed up to 200 km inshore of the FRIS ice front, where tidal mixing occurs (29). On average, nearby Weddell Sea Deep Waters (WDW) have warmed by 0.32°C since 1972 (16). In 2002, oceanographic measurements showed large quantities of modified WDW present in front of the northern Larsen-C (66.5°S) at depths well below the ice-shelf draft (300 m), with a potential temperature of −1.45 °C, that is, 0.65°C higher than the pressure melting point of ice (31). Elsewhere such differences generate up to 6.5 m yr^{-1} of basal ice melt (30) when water is delivered to the ice-shelf base.

The calving front of the Larsen-C has changed little in decades, and its flow geometry is considered to be stable (3). However, at the same time enhanced ocean melting has progressively thinned the shelf at its base. Thinning inevitably increases the ice-shelf exposure to crevasse fracture (7), and it is difficult to conclude that the thinning did not contribute toward either the creation of unstable conditions or the final disintegrations of the Larsen-A and -B sections. If our estimate of the basal erosion rate is correct, the Larsen-C will approach the thickness of the Larsen-B at the time of its collapse in some 100 years, more rapidly if the rate is increased by a warming ocean. It is possible that the LIS thinning provides a link between the regional climate warming and the disintegration of ice shelves at the Antarctic Peninsula.

References and Notes
1. D. G. Vaughan, C. S. M. Doake, *Nature* **379**, 328 (1996).
2. H. Rott, P. Skvarca, T. Nagler, *Science* **271**, 788 (1996).
3. C. S. M. Doake, H. F. J. Corr, H. Rott, P. Skvarca, N. W. Young, *Nature* **391**, 778 (1998).
4. J. H. Mercer, *Nature* **271**, 321 (1978).
5. H. Rott, W. Rack, T. Nagler, P. Skvarca, *Ann. Glaciol.* **27**, 86 (1998).
6. T. A. Scambos, C. Hulbe, M. Fahnestock, J. Bohlander, *J. Glaciol.* **46**, 516 (2000).
7. J. Weertman, International Association of Scientific Hydrology Publication **95**, 139 (1973).
8. D. J. Wingham, A. Ridout, R. Scharroo, R. Arthern, C. K. Shum, *Science* **282**, 456 (1998).
9. A. Shepherd, D. J. Wingham, J. A. D. Mansley, H. F. J. Corr, *Science* **291**, 862 (2001).
10. Changes in the electromagnetic properties of ice surfaces can affect the elevation recorded by a radar altimeter, and the shape of radar echoes reflects the degree of wave penetration (32). We examined radar echoes from the LIS in detail, and

they were almost identical to those reflected from an ocean surface. Analytical fits of a surface scattering model (33) to each time series of radar echoes yielded high correlation coefficients ($r^2 > 0.96$) in all instances. We detected no temporal change in the echoes and no penetration of the surface layer at any time.
11. Ocean tides generate up to 2.5 m of vertical motion at the LIS (34). Station data are too remote to produce tidal predictions for the entire LIS, and ocean tide solutions can prove inaccurate for ice shelves that do not respond freely to tidal forcing (35). We derived a model of the LIS tidal motion from the ERS altimeter data set itself (36) to estimate the displacement at the time and location of each elevation measurement. The same model resolved the four principal tidal constituents to within 10.9 cm of station records at the George VI Ice Shelf, ~500 km southeast.
12. W. Rack, thesis, Leopold-Franzens-Universitat (2000).
13. R. Warwick, C. Le Provost, M. Meier, J. Oerlemans, P. Woodworth, in *Climate Change 1995: The Science of Climate Change* (Cambridge Univ. Press, Cambridge, 1996), pp. 359–405.
14. J. R. Potter, J. G. Paren, M. Pedley, *British Antarctic Survey Bulletin* **68**, 1 (1985).
15. M. J. Whitehouse, J. Priddle, C. Symon, *Deep-Sea Research Part I–Oceanographic Research Papers* **43**, 425 (1996).
16. R. Robertson, M. Visbeck, A. L. Gordon, E. Fahrback, *Deep Sea Research* **49**, 4791 (2002).
17. J. C. Comiso, *Journal of Climate* **13**, 1674 (2000).
18. D. G. Vaughan, G. J. Marshall, W. M. Connolley, J. C. King, R. Mulvaney, *Science* **293**, 1777 (2001).
19. M. A. Fahnestock, W. Abdalati, C. A. Shuman, *Ann. Glaciol.* **34**, 127 (2002).
20. Firn density at the northern margin of the Larsen-B exceeds 838 kg m^{-3} at ~0.5 m depths (12). Detailed measurements on the George VI ice shelf, on the western coast of the AP, which has a melt season and temperature similar to those of the LIS, show values of ~900 kg m^{-3} in regions of melt ponding (similar to the northern LIS) and ~600 kg m^{-3} elsewhere (37). We use this latter value as a lower bound for the LIS surface density, the values measured in situ at the northern Larsen-B, and the latitudinal variation in annual melt-water production (22) to model the spatial variation in LIS surface firn density. This calculation gives surface density values of 893, 793, and 630 kg m^{-3} for the Larsen-A, -B and -C ice shelves, respectively.
21. N. Reeh, *Polarforschung* **59**, 113 (1991).
22. A comparison of surface ablation measurements recorded at five stakes (see Fig. 1) between 1996 and 2002 and positive degree-days recorded at meteorological stations to the north (Marambio) and south (Larsen) shows that average ablation equaled 2.8 ± 1.0 mm water-equivalent degree-day^{-1}. We used this factor and a positive degree-day model (21) to estimate changes in the mass of melted firn (table S1). Melt-water production was much larger at northerly latitudes.
23. M. B. Lythe, D. G. Vaughan, *J. Geophys. Res.* **106**, 11335 (2001).
24. More than 115,000 direct measurements of ice thickness have been recorded at the LIS on 11 separate occasions since 1966 (23). Absolute location and ice-thickness precision varied from 0.5 to 5000 m and 3 to 30 m, respectively, with older data showing the greatest uncertainty. We interpolated the entire 32-year, irregularly oriented ice-thickness data set onto a 500-m grid to facilitate coregistration and isolated more than 1000 separate locations where repeat measurements coincided. Some data were discarded in regions of high surface roughness. The 1966 to 1998 mean rate of thickness change of the Larsen-C ice-shelf was −0.29 ± 0.68 m yr^{-1}.
25. C. Raymond et al., *J. Glaciol.* **42**, 510 (1996).
26. J. Turner, S. Leonard, T. Lachlan-Cope, G. J. Marshall, *J. Glaciol.* **27**, 591 (1998).
27. W. S. B. Paterson, *The Physics of Glaciers* (Butterworth-Heinemann, Oxford, ed. 3, 1994).
28. K. Herterich, in *Dynamics of the West Antarctic Ice*

Sheet, C. J. Van der Veen, J. Oerlemans, Eds. (Reidel, Dordrecht, 1987).
29. I. Joughin, L. Padman, *Geophys. Res. Lett.* **30**, 1477 (2003).
30. E. Rignot, S. S. Jacobs, *Science* **296**, 2020 (2002).
31. K. Nicholls, personal communication.
32. J. K. Ridley, K. C. Partington, *International Journal of Remote Sensing* **9**, 601 (1988).
33. G. S. Brown, *IEEE Transactions of Antennas and Propagation* **25**, 67 (1977).
34. J. O. Speroni, W. C. Dragani, E. E. D'Onofrio, M. R. Drabble, C. A. Mazio, *Geoactas* **25**, 1 (2001).
35. N. Reeh, C. Mayer, O. B. Olesen, E. L. Christensen, H. H. Thomsen, *Ann. Glaciol.* **31**, 111 (2000).
36. A. Shepherd, N. R. Peacock, *J. Geophs. Res.* **108**, 3198 (2003).
37. C. S. M. Doake, *Ann. Glaciol.* **5**, 47 (1984).
38. J. G. Ferrigno *et al.*, AVHRR Antarctic Mosaic (USGS I-2560, 2001).
39. Supported by the United Kingdom Natural Environment Research Council Centre for Polar Observation and Modelling and Instituto Antártico Argentino. We thank the European Space Agency for ERS data and the British Antarctic Survey for access to the BEDMAP database.

Carbonate Deposition, Climate Stability, and Neoproterozoic Ice Ages

Andy J. Ridgwell,[1]* Martin J. Kennedy,[1] Ken Caldeira[2]

The evolutionary success of planktic calcifiers during the Phanerozoic stabilized the climate system by introducing a new mechanism that acts to buffer ocean carbonate-ion concentration: the saturation-dependent preservation of carbonate in sea-floor sediments. Before this, buffering was primarily accomplished by adjustment of shallow-water carbonate deposition to balance oceanic inputs from weathering on land. Neoproterozoic ice ages of near-global extent and multimillion-year duration and the formation of distinctive sedimentary (cap) carbonates can thus be understood in terms of the greater sensitivity of the Precambrian carbon cycle to the loss of shallow-water environments and CO_2-climate feedback on ice-sheet growth.

The growth of continental-scale ice sheets extending to the tropics during the second half of the Neoproterozoic (1000 to 540 million years ago) (*1*) is now widely accepted in the geological community and has been of particular interest because of its close stratigraphic association with the first appearance of metazoans and the possibility that ice ages served as an environmental filter for animal evolution (*2*). The severity of these ice ages, which may record the coldest times in Earth history (*3*), implies that the Precambrian climate system must have operated very differently from today. This is supported by the ubiquitous occurrence of thin post-glacial "cap" carbonate units (*4–7*), apparent perturbations of the carbon cycle that did not recur in the Phanerozoic. To account for these observations, we focus on a first-order difference between the Precambrian and modern Earth systems and its implications for atmospheric CO_2: the absence of a well-developed deep-sea carbonate sink before the proliferation of calcareous plankton.

On the time scale of glaciations ($\sim10^4$ to 10^6 years), the balance between weathering of terrigenous rocks and the burial flux of calcium carbonate ($CaCO_3$) in marine sediments exerts a key control on ocean carbonate chemistry (*8*), with this burial today divided roughly equally between deep-water (pelagic) and shallow-water (neritic) zones (*9*). The latter sink is of particular relevance in the context of ice ages, because the total neritic area available for $CaCO_3$ burial is highly sensitive to sea level, a consequence of the nonuniform distribution of the Earth's surface area with elevation (Fig. 1). The climatic relevance arises because any increase in the carbonate ion concentration ($[CO_3^{2-}]$) at the ocean surface will induce lower atmospheric CO_2 (because the aqueous carbonate equilibrium, $CO_2 + CO_3^{2-} + H_2O \leftrightarrow 2HCO_3^-$, is shifted to the right). This is the basis for the coral reef hypothesis for Quaternary glacial-interglacial CO_2 control (*10–13*), in which lowered sea level reduces available neritic area and $CaCO_3$ accumulation rates, driving higher $[CO_3^{2-}]$ and lower CO_2.

We have identified a fundamental difference between ancient and modern carbon cycles in the relative importance of the neritic carbonate sink that would make the impact of a coral reef–like effect much greater in the Precambrian. In the modern system, higher $[CO_3^{2-}]$ enhances the preservation of carbonate in deep-sea sediments; hence, a reduction in neritic carbonate deposition due to a fall in sea level can be compensated for by a greater burial flux in deep-sea sediments of $CaCO_3$ that originates from planktic calcifiers (*9*) (Fig. 1). This provides a strong negative (stabilizing) feed-back on the modern carbon cycle, restricting oceanic $[CO_3^{2-}]$ variation and thus limiting the atmospheric response to sea level change.

The Neoproterozoic carbon cycle, by contrast, did not possess this stabilizing feedback, because before the advent of pelagic calcifiers in the Cambrian and the subsequent proliferation of coccolithophores and foraminifera during the Mesozoic (*14*), carbonate deposition would have been largely limited to neritic zones. The importance of the calcareous plankton that dominate carbonate deposition in the modern open ocean (*9*) is illustrated by the comparative rarity of deep-sea pelagic carbonate material in ophiolite suites older than ~300 million years (*14*). As neritic carbonate deposition was the dominant mechanism of CO_3^{2-} removal in the Precambrian ocean, it follows that atmospheric CO_2 would have been much more sensitive to sea level change. We explore the implications for the Neoproterozoic carbon cycle of sea level variation with the aid of a numerical model (*15*). This model calculates the evolution in atmospheric CO_2 that arises from a reduction in the area available for neritic carbonate deposition.

Although these observational and evolutionary arguments suggest a highly limited role for the deep-sea carbonate buffer in the Precambrian carbon cycle, Precambrian ocean chemistry would instead have been stabilized by the dependence of shallow-water carbonate deposition rates on $[CO_3^{2-}]$ (*8*). As oceanic $[CO_3^{2-}]$ (and saturation state, Ω) rises after a fall in sea level, the smaller area available for carbonate deposition is eventually compensated for by a higher precipitation rate per unit area. An analogous compensating increase in the neritic $CaCO_3$ precipitation rate may have occurred at the Cretaceous/Tertiary boundary after the extinction-driven reduction of pelagic carbonate productivity (*8*). The precipitation rate of carbonate minerals is expressed in the model as a proportionality with $(\Omega - 1)^n$ (*16*), where Ω is defined as $([Ca^{2+}] \times [CO_3^{2-}])/K_{sp}$ (where K_{sp} is a solubility constant). The parameter n is a measure of how strongly $CaCO_3$ precipitation rate responds to a change in ambient $[CO_3^{2-}]$ and thus of how effectively ocean chemistry and atmospheric CO_2 are buffered. Possible values range from ~1.0 for modern biological systems such as corals (*17*) to $1.9 \leq n \leq 2.8$ for precipitation that occurs under entirely abiotic conditions (*16*). We therefore initially set $n = 1.7$ (*8, 11*). Because $CaCO_3$ precipitation dur-

[1]Department of Earth Sciences, University of California–Riverside, Riverside, CA 92521, USA. [2]Climate and Carbon Cycle Modeling Group, Lawrence Livermore National Laboratory, 7000 East Avenue, L-103, Livermore, CA 94550, USA.

*To whom correspondence should be addressed. E-mail: andyr@citrus.ucr.edu

ERRATUM

post date 12 March 2004

REPORTS: "Larsen Ice Shelf has progressively thinned" by A. Shepherd *et al.* (31 Oct. 2003, p. 856). There were two errors in the printed form of equation (1): an incorrect expression of the density-related factor of the mass fluctuation terms and an incorrect expression of the mass flux divergence. The correct equation, which the authors used in their analysis, appears below.

$$\frac{\partial h}{\partial t} = \frac{\partial \Delta_s}{\partial t} - M \frac{\partial}{\partial t}\left(\frac{1}{\rho_w}\right) + \int_0^M dm \frac{\partial}{\partial t}\left(\frac{1}{\rho_f(m)}\right) + \left(\frac{1}{\rho_{ice}} - \frac{1}{\rho_w}\right)\left(\dot{M}_s + \dot{M}_b + \nabla.(Mv)\right)$$

The authors thank David Holland for bringing these errors to their attention.